Solution flow rate influence on ZnS thin films properties grown by ultrasonic spray for optoelectronic application

Article *in* Journal of Semiconductors · September 2018

DOI: 10.1088/1674-4926/39/9/093001

CITATION
1

READS
286

9 authors, including:

Derbali Ammar
Université de Biskra
5 PUBLICATIONS **12** CITATIONS
SEE PROFILE

Hanane Saidi
Mohamed Khider University
42 PUBLICATIONS **211** CITATIONS
SEE PROFILE

Abdallah Attaf
Université de Biskra
52 PUBLICATIONS **344** CITATIONS
SEE PROFILE

A. Bouhdjer
Université Batna 2
25 PUBLICATIONS **137** CITATIONS
SEE PROFILE

Solution flow rate influence on ZnS thin films properties grown by ultrasonic spray for optoelectronic application

A. Derbali[a], H. Saidi[a], A. Attaf[a], H. Benamra[a], A. Bouhdjer[a], N. Attaf[b], H. Ezzaouia[c], L. Derbali[c], and M.S. Aida[d]

[a]Laboratory of Thin Films and Applications LPCMA, University of Biskra, Algeria, BP 145 RP, 07000 Biskra, Algérie
[b]Laboratoire de Couches Minces et Interfaces Faculté des Sciences Université de Constantine, Algeria
[c]Laboratory of Semiconductors, Nanostructures and Advanced Technology (LSNTA), Research and Technology Centre of Energy, Borj-Cedria Science and Technology Park, BP 95, 2050 Hammam-Lif, Tunisia
[d]Department of physics faculty of sciences, King abdulaziz university, Djeddah, KSA

Abstract: The aim of this work is to investigate the dependence of ZnS thin films structural and optical properties with the solution flow rate during the deposition using an ultrasonic spray method. The solution flow rate ranged from 10 to 50 mL/h and the substrate temperature was maintained at 450 °C. The effect of the solution flow rate on the properties of ZnS thin films was investigated by X-ray diffraction (XRD), scanning electron microscopy (SEM), optical transmittance spectroscopy (UV-V) and the four-point method. The X-ray diffraction analysis showed that the deposited material was pure zinc sulphide, it has a cubic sphalerite structure with preferential orientation along the (111) direction. The grain size values were calculated and found to be between 38 to 82 nm. SEM analysis revealed that the deposited thin films have good adherence to the substrate surfaces, are homogeneous and have high density. The average transmission of all films is up more than 65% in the range wavelength from 200 to 1100 nm and their band gap energy values were found between 3.5–3.92 eV. The obtained film thickness varies from 390 to 1040 nm. Moreover, the electric resistivity of the deposited films increases with the increasing of the solution flow rate between 3.51×10^5 and 11×10^5 Ω·cm.

Key words: zinc sulphide; X-ray diffraction; ultrasonic spray; solution flow rate; optical and electrical properties
DOI: 10.1088/1674-4926/39/9/000000 **EEACC:** 2520

1. Introduction

Zinc sulphide (ZnS) is a semiconductor material with a large direct band gap between 3.4–3.70 eV depending upon composition[1–2]. ZnS thin films have attracted the interest of many researchers during the last few years, due to their potential applications in the industrial domain, especially optoelectronic devices. In comparison with CdS, Zinc sulphide (ZnS) is the most promising compound that plays an important role in the area of optoelectronic and photovoltaic applications, because of many advantages including: it has a transparent semiconductor, a wide gap, is non toxic, environmentally safe and exists on earth abundantly[3]. These advantages can be utilised in several applications such as: thin film solar cells, light emitting diodes and electroluminescent devices[4], antireflection coatings and optical filters[5]. There are many techniques such as pulsed-laser deposition (PLD), sputtering[6], chemical vapour deposition (CVD)[7], molecular beam epitaxial (MBE)[8], atomic layer epitaxial (ALE)[9], thermal evaporation[10], as well as spray pyrolysis[11], sol-gel[12], electro-deposition[13] and chemical bath deposition (CBD)[14] have been used to fabrication ZnS thin films. However, compared to the other deposition method, ultrasonic spray is widely used for the synthesis of nano-materials and high quality thin films and known as the most suitable method for preparing thin layers of ZnS, due to it beingeconomical, simple, feasible, flexible, cost effective, convenient for large-area deposition at low temperatures and it allows easy deposition in the atmospheric condition. Further, there are several factors that mainly affect the basic properties of the deposited thin films by this technique such as the deposition time, solution flow rate, substrate temperature, distance nozzle-substrate etc.

In this work, we investigate the effect of solution flow rate on the structural, optical and electrical properties of ZnS thin films prepared by ultrasonic spray technique at 450 °C. Obtained results prove the beneficial effect of this varied parameter. The prepared thin films can be used as an alternative to cadmium sulphide (CdS) and as a buffer layer in CIGS solar cells.

2. Experimental details

The deposition system is a special setup prepared in the laboratory as shown in Fig. 1. The nozzle is fed by the solution content in the syringe pump, which is controlled by a push syringe device (to control the infusion flow rate solution) and the incoming liquid is atomized by ultrasonic wave (40 kHz) derived from a generator (Sonics vibra-cell). The obtained stream is formed by very small and uniform droplets with diameter around 40 μm. ZnS thin films were deposited on glass substrates with dimensions of 25 × 15 mm^2 at 450 °C using the ultrasonic spray technique. Prior to the deposition, the glass substrates were treated in standard cleaning as follows: rinsed in acetone and ethanol for 10 min to remove

Received 9 December 2017, revised manuscript received 14 February 2018

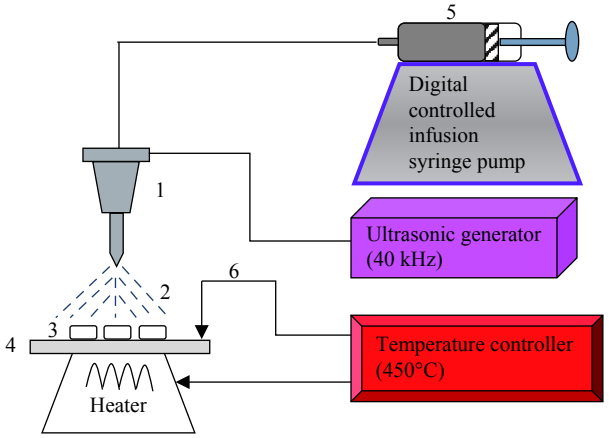

Fig. 1. (Color online) Experimental set up schematic of the used spray deposition system. 1- Spray nozzle. 2- Droplets stream. 3- Substrate. 4- Substrate holder. 5- Syringe (container of solution). 6- Thermocouple K.

Table 1. Deposition parameters used to prepare the ZnS thin film by spray ultrasonic.

Deposition parameter	Corresponding value
Solution quantity	30 ml
Substrate - nozzle distance	50 mm
Substrate temperature	450 °C
Molarity of solution	0.1 M
Deposition time	6 min
Solution flow rate	10, 20, 30, 40, 50 mL/h

grease, then washed in distilled water to remove the impurities and residuals from substrate surfaces, finally they were dried with compressed air. The starting solution was prepared by dissolving zinc chloride ($ZnCl_2$) and thiourea ($SC(NH_2)_2$) with 0.1 M concentration in 30 ml of methanol CH_3OH and it was stirred thoroughly using a magnetic stirrer at room temperature for 2 h to obtain a complete homogeneity and transparent solution. The solution was sprayed over the heated substrate held at constant temperature. The deposition parameters of ZnS thin films were all kept constant such as: the substrate temperature was 450 °C, the deposition time was fixed at 6 min, and the distance nozzle-substrate was fixed at 50 mm. The solution flow rate was varied from 10 to 50 mL/h with a step of 10 mL/h.

The deposition parameters are summarized in Table 1. Commonly, when the solution droplets reach the heated substrate surface the following chemical reaction occurs:

$$ZnCl_2 + CS(NH_2)_2 + CH_3OH + \frac{3}{2}O_2 \rightarrow ZnS + 2NH_4Cl(gas) + 2CO_2(gas)$$

According to this reaction, a ZnS thin film should be formed onto the glass substrate surface and the $2NH_4Cl$, CO_2 leaves the system as gas.

The structural, optical and electrical characterization of all the films were treated by many techniques. The crystalline structure of the film was characterized using an X-ray diffracto-meter (D8 ADVANCED BRUKER) with Cu-Kα radiation (λ = 1.5418 Å) within the 2θ range of 10°–70°. The surface morphology of the obtained thin films was studied using a VEGAS3 TESCAN scanning electron microscope. The optical transmittance was measured at room temperature using an UV-Vis spectrophotometer (PerkinElmer LAMBDA1050). The electrical resistivity was measured at room temperature via the four-probe method, using the JANDEL RM 3000 device.

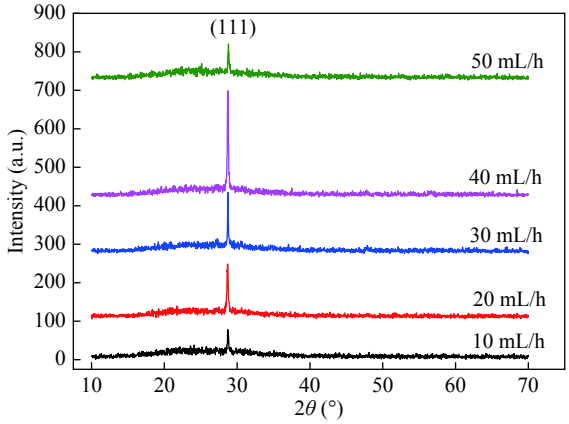

Fig. 2. (Color online) XDR pattern of ZnS films deposited at different solution flow rate.

3. Results and discussion

3.1. Structural properties:

Zinc sulphide exists in sphalerite, cubic (zinc blende) and hexagonal (wurtzite) forms. The cubic form is stable at room temperature, while the less dense hexagonal form is stable at above 1020 °C at atmospheric pressure[15]. The XRD pattern of all ZnS films prepared at different solution flow rates at the same substrate temperature (450 °C) are shown in Fig. 2. Grown films at various solution flow rates show only one preferential orientation along the (111) direction at 2θ = 28, 75 ° indicating a cubic structure (JCPDS card N°: 55-0566). The (111) planes are the closest-packed ones for the cubic sphalerite structure. No other peaks related to hexagonal phases or the oxidation phases (ZnO) are seen in the XRD spectra, confirming the stoichiometric of ZnS thin films. From the XRD analysis we found that the (111) peak has a high intensity, this is due to two reasons: first, the (111) plane has the lowest surface energy[16], ascribed to the highest atomic density achieved along the (111) direction; second, that the (111) plane was parallel to the substrate surface[17]. The preferential orientation (111) was reported by several authors [18–20]. As also observed in Fig. 2, that the intensity of the (111) peak increases gradually as the solution flow rate goes up to 40 mL/h, then decreases again when the solution flow rate increases. The latter indicates an improved crystallinity of the obtained films, which can be ascribed to the increased thickness of ZnS films for a solution flow rate lower than 50 mL/h and the crystallinity decreases for 50 mL/h. Moreover, we notice that there is a small difference in the position of the ZnS (111) diffraction peak (variation in the value of the angle diffraction 2θ) that is probably caused by the manifestation of the stress during the films growth.

Table 2. Calculated lattice constant (a) from XRD pattern at different solution flow rates.

Solution flow rate (mL/h)	*hkl* planes	2θ (degree)	Calculated parameters		Reference parameter (JCPDS card No 05-0566)
			a (Å)	d (Å)	
10	(111)	28.74	5.379	3.1055	
20	(111)	28.68	5.383	3.108	
30	(111)	28.74	5.386	3.1095	a = 5.406 Åd = 3.123 Å
40	(111)	28.72	5.39	3.112	
50	(111)	28.80	5.369	3.1	

Table 3. Structural parameters of chemically deposited ZnS thin films at different solution flow rates.

Solution flow rate(mL/h)	**(*hkl*)**	**2θ (degree)**	**FWHM (degree)**	***D* (nm)**	**δ(10^{14} lines/m^2)**	**ε(10^{-4})**
10	(111)	28.74	0.216	38	6.93	9.425
20	(111)	28.68	0.144	57	3.08	6.28
30	(111)	28.74	0.108	76	1.73	4.71
40	(111)	28.72	0.1	82	1.48	4.36
50	(111)	28.80	0.2	41	5.94	8.73

The lattice constant (a) for the cubic phase of ZnS is determined by the expression given by Eq. (1)[21]:

$$a = d\left(h^2 + k^2 + l^2\right)^{\frac{1}{2}}, \quad (1)$$

where h, k and l denote the lattice planes. The inter-planar spacing d is evaluated using the standard Bragg relation (Eq. (2)):

$$d = \frac{n.\lambda}{2\sin\theta}, \quad (2)$$

where θ is the diffraction angle and λ is the X-ray wavelength (1.5418 Å).

In Table 2 we present a summary of the calculation lattice constant (a) from the XRD pattern of the ZnS thin films at different solution flow rates.

The resulting changes in the lattice parameter value are related to the intrinsic stress developed in the ZnS crystal lattice.

The crystallite size of ZnS was estimated by using the well-known Debye-Scherer equation[22]:

$$D = \frac{0.94\lambda}{\beta\cos\theta}, \quad (3)$$

where λ is the used radiation wavelength (λ = 1.5418 Å), θ is the diffraction angle of the concerned diffraction peak, and β is the full width at half maximum (FWHM) of the diffraction peak corresponding to a particular crystal plane.

Using crystallite size values and the formula of Williamson and Smallman[23] (Eq. (4)) we can determine the dislocation density (δ) that represented the length of dislocation lines per unit volume:

$$\delta = \frac{1}{D^2}. \quad (4)$$

The micro strains (ε) of films were estimated using the equations[24]:

$$\varepsilon = \frac{\beta\cos\theta}{4}. \quad (5)$$

The calculated values of crystallite size, dislocation and strain are presented in Table 3.

Table 3 shows obviously the dependence of the crystallite size with the variation of the solution flow rate during the deposition. The crystallite size was found to increase with increasing the flow rate between 10 and 40 mL/h. The individual final sizes of the nanocrystallites depend on the number of nucleation points. The solute atoms of the liquid spread along the substrate surface and begin to bind to one another at the nucleation points and form clusters. The size of the crystals increases because the nucleation density points augment due to the increased solute atoms arriving at the substrate surface, until it touches the neighbouring nanocrystallites, which means with increasing the solution flow rate the nuclei size growth is faster than the growth rate of the films, hence the nanocrystallites sizes become larger. Imen Bouhaf *et al.*[25] have found that the average crystallite size between 7.26 to 19.36 nm with variation of flow rates and the similar increasing of grain size between 19 to 67 nm has been obtained by Bouhdjer *et al.*[26]. Above the value of 40 mL/h the grain size is reduced with increasing of the solution flow rate. This indicates the deterioration of the film crystallinity because the orientation (111) was decreased and this can be due to an increase of defects density in the film network, enabling the rise of internal strain in the formed crystallites. Valenzuela and Russer reported that the FWHM of an XRD peak is reliant on the crystallite size and the lattice strain caused by the defect and/or dislocations[27].

The dislocation density varied between 1.48 × 10^{14} and 6.93 × 10^{14} lines/m^2, due to the edge of a crystal or a grain boundary, which mean the grain boundary is a dislocation trap.

3.2. Surface morphology:

The surface morphology of ZnS thin films prepared at different solution flow rates is shown in Fig. 3.

Evidently from Fig. 3 we conclude that the prepared thin films have the same morphology and good adherence to the substrate surfaces, the thin films display a homogenous, uniform and dense without crack and pin holes surface. As also

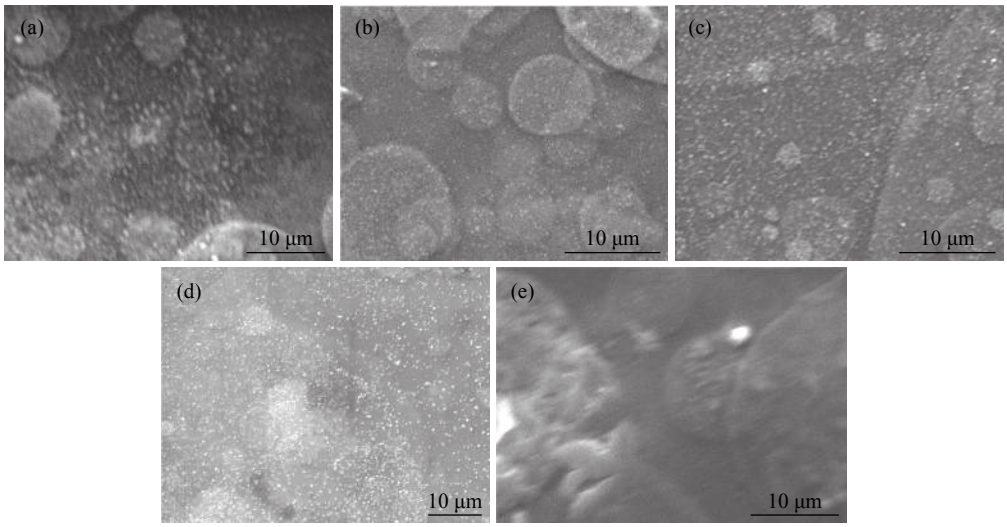

Fig. 3. Scanning electron microscopy of ZnS thin films deposited at various solution flow rates: (a) 10 mL/h, (b) 20 mL/h, (c) 30 mL/h, (d) 40 mL/h, and (e) 50 mL/h.

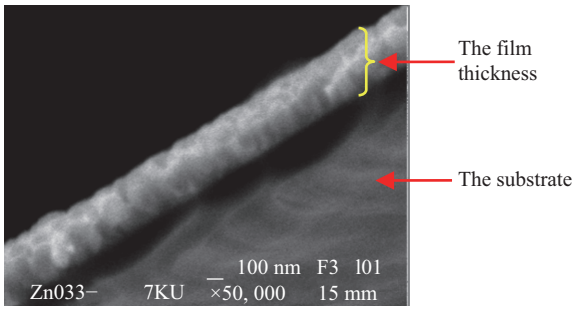

Fig. 4. (Color online) Direct thickness measurement of the film of ZnS from the cross sectional SEM images.

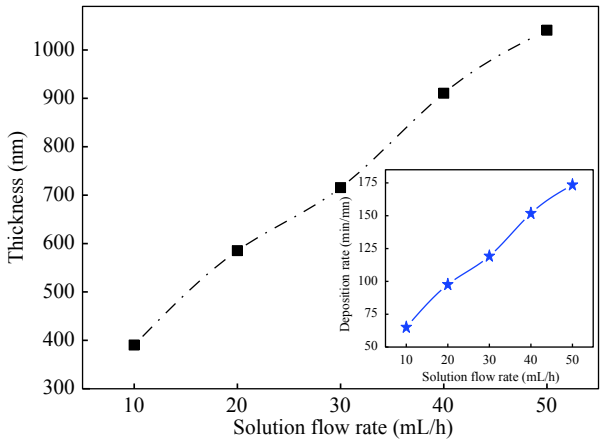

Fig. 5. (Color online) Film thickness and deposition rate as a function of solution flow rate.

seen in Fig. 3, the surface is covered with grains having a disk-like form with different size in all scanned areas of the samples and along the surface become larger with increasing the solution flow rate, which agree with XRD results. Moreover, larger grain sizes raise the film surface roughness causing an enhancement in the optical transmittance, and this is what makes these films suitable for potential applications in optoelectronic devices.

3.3. Optical properties:

The film thickness of ZnS films deposited at various solution flow rates was determined using the cross sectional SEM images shown in Fig. 4.

Fig. 5 shows the variation of the film thickness as a function of the solution flow rate. It is shown that the increased solution flow rate results in an apparent rise of the film thickness from 390 nm (10 mL/h) to 1040 nm (50 mL/h). Obtained thickness values are in good agreement with earlier reported works[28]. The highest growth rate is obtained for the film deposited with 50 mL/h, which is equal to 173 nm/min. Otherwise, the smallest growth rate equal to 65 nm/min corresponded to 10 mL/h of the solution flow rate. The increase in the deposition rate with varying the solution flow rate is suggested to be due to the increase in the kinetics of reactions during the growth of the films, which are activated thermally by means of the controlled substrate surface temperature, this allows the incoming species on the surface substrate to have enough time to find a favorable site and to form a more organized material. The resulting film thickness variation can be attributed to the increase of the amount of flow rate droplets reaching the surface substrate, hence bringing a large quantity of ingredient ions and solute atoms from the atomizer to the surface of the substrate with the increased solution flow rate. A similar increase in the film thickness has been reported by Gangopadhyay *et al*.[29] for ZnS thin films prepared by chemical bath deposition.

The optical transmittance of the deposited ZnS films at different solution flow rate has been measured at room temperature by an UV/VIS spectrophotometer, as shown in Fig. 6, in the wavelength region of 300–1100 nm.

The spectral transmittance curves indicate a high transmission for an average transmittance of 65–77% in the visible range, which is what makes it very appropriate to be used as a dielectric filter in the area of optics. These values were reported by several authors[30, 31]. According to Fig. 6, we conclude that the transparency of the prepared films decreased slightly after increasing the solution flow rate, this can be attrib-

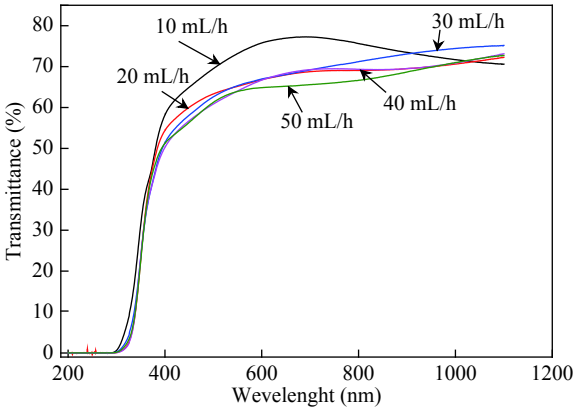

Fig. 6. (Color online) Transmission spectra of ZnS films deposited at different solution flow rates.

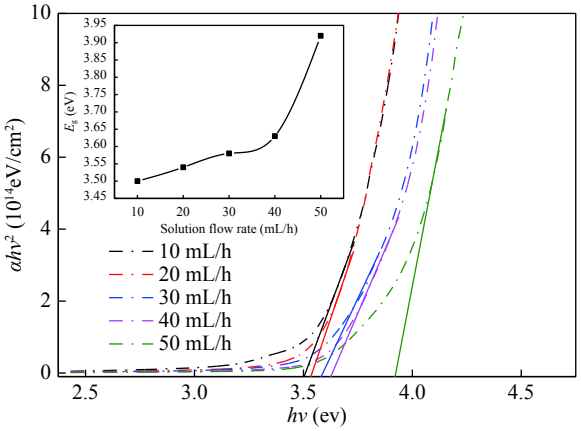

Fig. 7. (Color online) Band gap energy of the ZnS films as a function of solution flow rate.

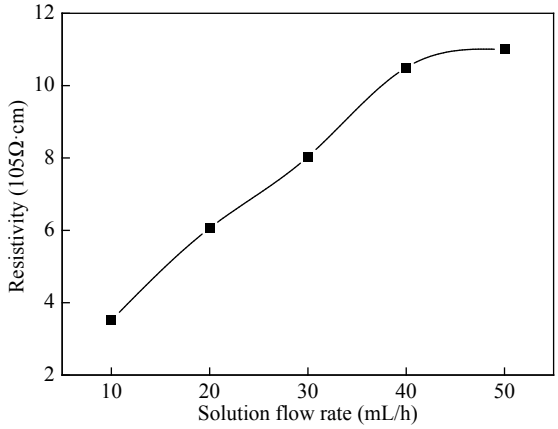

Fig. 8. Variation in electrical resistivity of the ZnS thin films at different solution flow rates.

uted to the increase in films thickness. The same observation was obtained by Benkhetta[32]. Furthermore, we notice the absence of interference fringes that may be due to the multiple reflections on the levels of the interfaces film/substrate and to film/air. So the absence of these fringes in our films indicates a roughness of free surface of ZnS films, which causes scattering of incident light on the material[33]. As we can see an abrupt fall of the transmission for the wavelengths less than 380 nm, which corresponds to strong absorption in ZnS following the transition between the valence band (VB) and the conduction band (CB). This last phenomenon is a very important characteristic for a semiconductor, which corresponds to the optical band gap energy (E_g).

The optical band gap of a semiconductor material can be obtained after drawing the curve of a tuk relationship[34]:

$$\alpha h\nu = K\left(h\nu - E_g\right)^n, \tag{6}$$

where E_g is the optical band gap, K is a constant and $h\upsilon$ is the photon energy. The index n characterizes the transition between the valence and the conduction bands. For a direct band gap semiconductor, n is $^1/_2$. The band gap energy (E_g) is determined by extrapolating the straight line portion of the spectrum to $\alpha h\upsilon = 0$. Fig. 7 shows the band gap energy of the ZnS films as a function of the solution flow rate.

It can be observed that the band gap slightly increases from 3.5 to 3.63 eV between 10 and 40 mL/h solution flow rates. This increase in the band gap energy (E_g) values may be attributed to the Moss-Burstein effect caused by the increase in the film thickness. According to Brustein and Moss[35] this difference is due to an increase in the charge carriers in the band of conduction. The slight increase of gap optic is a consequence of the convergence of the changing grains size values. Between the 40 and 50 mL/h flow rates the band gap energy increase quickly from 3.63 to 3.92 eV, due to the quantum size effects owing to the decrease in particle size[36] as shown in Tables 3; as a result there is an increase of the grain boundary, which indicates the increasing of defects density and impurities in the ZnS thin film network. These values of the band gap energies are in good agreement with the reported values in other reports in the literature [37-39]. The widening band gap energy makes these films one of the most important candidates for use as a light emitting diode (LED) and the window layer in photovoltaic solar cells, this is due to decreases in the window absorption losses and that will cause an increase in the short circuit current[40].

3.4. Electrical properties

The resistivity of our ZnS thin films was calculated according to Eq. (7)[41]:

$$\rho = R_S d, \tag{7}$$

where ρ is the resistivity, R_S is the square resistance ($R_S = \frac{\pi}{ln2}\cdot\frac{U}{I}$, U is the voltage and I is the current) and d is the films thickness. The values of the electric resistivity as a function of the solution flow rate can be shown in Fig. 8.

As it is observed in Fig. 8, the resistivity was increased from 3.51×10^5 to 11×10^5 Ω·cm with increasing of the solution flow rate. These variations are less than those reported before[42, 43] and are in good agreement with the previous obtained results[28]. Some physical variations such as crystal structure, carrier concentration, mobility and grain size are controlled by the films resistivity. This increase in resistivity is due to the decreases of disorder in the films network, this decrease in disorder yields to the enhancement of the film homo-

geneity, while on the other hand the diminution of Zn atoms in the interstitial site, causing the reduction of free carriers concentration and subsequently the film resistivity rises. The increasing of the resistivity can be explained also by the effect of films thickness, the electrical resistivity in semiconductors is proportional to the film thickness, as seen in Eq. (7).

4. Conclusion

In this work, the effects of solution flow rate on the structural, optical and electrical properties of ZnS thin films deposited by ultrasonic spray were investigated. The XRD measurements reveal that the crystallinity of the films can be improved using a solution flow rate up to 40 mL/h with strongly (111) preferred orientation. The average grain size is around 58.82 nm. The resistivity was found in the range of 3.51×10^5–11×10^5 Ω·cm. The film thickness increases from 390 to 1040 nm with increasing solution flow rate. Obtained results promise a potential application of ultrasonic spray deposited ZnS thin films for the solar cells.

These produced films could be useful for applications as transparent windows in solar cells or other optoelectronic devices. For example, a stoichiometric ZnS in CIGS solar cell as a buffer layer strongly increases the CIGS cell efficiency by the alteration in the electronic structure at the ZnS/CIGS interface, moreover, the ZnS has a wider energy band gap, which transmits even higher energy photons and increases the light absorption in the absorber layer.

Finally, the solution flow rate is an important and sensitive factor for controlling the quality of the ZnS thin films deposited by ultrasonic spray technique.

References

[1] Meshram R S, Thombre R M. Structural and optical properties of ZnS thin films deposited by spray pyrolysis technique. International Conference on Benchmarks in Engineering Science and Technology ICBEST, 2012

[2] Shinde M S, Ahirrao P B, Patil R S . Structural, optical and electrical properties of nanocrystalline ZnS thin films deposited by novel chemical route. Archives Appl Sci Res, 2011, 3(2): 311

[3] Subbaiah Y P V, Prathap P, Ramakrishna Reddy K T. Structural, electrical and optical properties of ZnS films deposited by close-spaced evaporation. Appl Surf Sci, 2006, 253: 2409

[4] Xue S W, Chen J, Zou C W. Preparation and characterization of cubic lattice ZnS:Na films with (111) preferred orientation. Optoelectron Lett, 2014, 10: 0206

[5] Ashraf M, Akhtar S M J, Alia Z, et al. the influence of substrate temperature on the structural and optical properties of zns thin films. Semiconductors, 2011, 45: 699

[6] Liu T Z, Ke H, Zhang H, et al. Effect of four different zinc salts and annealing treatment on growth, structural, mechanical and optical properties of nanocrystalline ZnS thin films by chemical bath deposition. Mater Sci Semicond Process, 2014, 26: 301

[7] Khalifa Z S, Mahmoud S A. Photocatalytic and optical properties of titanium dioxide thin films prepared by metalorganic chemical vapordeposition. Physica E, 2017, 91: 60

[8] Zhang L, Szargan R, Chasse T. Electron-diffraction and spectroscopical characterisation of ultrathin ZnS films grown by molecular beamepitaxy on GaP(0 0 1). Appl Surf Sci, 2004, 227: 261

[9] Ku C S, Huang J M, Lin C M, et al. Fabrication of epitaxial ZnO films by atomic-layer deposition with interrupted flow. Thin Solid Films, 2009, 518: 1373

[10] Dimitrova V, Tate J. Synthesis and characterization of some ZnS-based thin film phosphors for electroluminescent device applications. Thin Solid Films, 2000, 365(1): 134

[11] Kriisa M, Kiirber E, Krunks M, et al. Growth and properties of ZnO films on polymeric substrate by spray pyrolysis method. Thin Solid Films, 2014, 555: 87

[12] Tang W, Cameron D C. Electroluminescent zinc sulphide devices produced by sol-gel processing. Thin Solid Films, 1996, 280: 221

[13] Baranski A S, Fawcett W R, McDonald A C. The mechanism of electrodeposition of cadmium sulphide on inert metals from dimethylsulphoxide solution. Journal of Electroanalytical Chemistry and Interfacial Electrochemistry, 1984, 160: 271

[14] Dona J M, Herrero J. Chemical bath codeposited CdS/ZnS film characterization. Thin Solid Films, 1995, 5: 268

[15] Nabiyouni G, Sahraei R, Toghiany M, et al. preparation and characterization of nanostructured ZnS thin films grown on glass and n-type Si substrates using a new chemical bath deposition technique. Rev Adv Mater Sci, 2011, 27: 52

[16] Yoshiyama H, Tanaka S, Mikami I, et al. Role of surface energy in the thin film growth of electroluminescent ZnS, CaS, and SrS. J Cryst Growth, 1988, 86: 56

[17] Kucukomeroglu T, Bacaksiz E, Terzioglu C, et al. Influence of fluorine doping on structural, electrical and optical properties of spray pyrolysis ZnS films. Thin Solid Films, 2008, 516: 2913

[18] Xue S W. Effects of thermal annealing on the optical properties of ar ion irradiated ZnS films. Ceram Int, 2013, 39(6): 6577

[19] Jin C, Kim H, Baek K, et al. Effects of coating and thermal annealing on the photoluminescence properties of ZnS/ZnO one-dimensional radial heterostructures. Mater Sci Eng B, 2010, 170: 143

[20] Zhang Z Z, Shen D Z, Zhang J Y, et al. The growth of single cubic phase ZnS thin films on silica glass by plasma-assisted metalorganic chemical vapor deposition. Thin Solid Films, 2006, 513: 114

[21] Subbaiah Y P V, Prathap P, Reddy K T R. Structural, electrical and optical properties of ZnS films deposited by close-spaced evaporation. Appl Surf Sci, 2006, 253: 2409

[22] Bendjedidi H., Attaf A., Saidi H., Aida M. S., Semmari S., Bouhdjar A., and Benkhetta Y. Properties of n-type SnO_2 semiconductor prepared by spray ultrasonic technique for photovoltaic applications. Journal of Semiconductors, 2015, 36(12)

[23] Kherchachi I. B., Attaf A., Saidi H., Bouhdjer A., Bendjedidi H., Benkhetta Y., and Azizi R. Structural, optical and electrical properties of Sn_xS_y thin films grown by spray ultrasonic. Journal of Semiconductors, 2016, 37

[24] Attaf A., Bouhdjer A., Saidi H., Aida M.S., Attaf N., Ezzaoui H. On tuning the preferential crystalline orientation of spray pyrolysis deposited indium oxide thin films. Thin Solid Films, 2017, 625: 177

[25] Kherchachi I B, Saidi H, Attaf A, et al. Influence of solution flow rate on the properties of SnS2 films prepared by ultrasonic spray. Optik, 2016, 127: 4043

[26] Bouhdjer A, Saidi H, Attafa A, et al. Structural, morphological, optical, and electrical properties of In_2O_3 nanostructured thin films. Optik, 2016, 127: 7319

[27] Valenzuela A A, Russer P. High Q coplanar transmission line resonator of $YBa_2Cu_3O_{7-x}$ on MgO. Appl Phys Lett, 1989, 55: 1029

[28] Erken O, Gunes M, Ozaslan D et al. Effect of the deposition time on optical and electrical properties of semiconductor ZnS thin films prepared by chemical bath deposition. Ind J Pure Appl Phys, 2017, 55: 471
[29] Gangopadhyay U, Kim K, Dhunge S K, et al. Application of CBD-Zinc Sulfide Film as an Antireflection Coating on Very Large Area Multicrystalline Silicon Solar Cell. Adv Opto-Electrons, 2011, 2007: 1687
[30] Sartale S D, Sankapal B R, Lux-Steiner M, et al. Preparation of nanocrystalline ZnS by a new chemical bath deposition route. Thin Solid Films, 2005, 168: 480
[31] Antony A, Murali K V, Monoj R, et al. The effect of the pH value on the growth and properties of chemical-bath-deposited ZnS thin films. Mater Chem Phys, 2005, 90: 106
[32] Benkhetta Y, Attaf A, Saidi H, et al. Influence of the solution flow rate on the properties of zinc oxide(ZnO) nano-crystalline films synthesized by ultrasonic spray process. Optik, 2016, 127: 3005
[33] Derbali A, Attafa A, Saidi H, et al. Investigation of structural, optical and electrical properties of ZnS thin films prepared by ultrasonic spray technique for photovoltaic applications. Optik, 2018, 154: 286
[34] Bouaichia F, Saidi H, Attaf A, et al. The synthesis and characterization of sprayed ZnO thin films: As a function of solution molarity. Main Group Chem, 2016, 15: 57
[35] Sahal M, Hartiti B, Mari B, et al. Etude des propriétés physiques des couches minces de ZnO dopées Al, préparées par la méthode de « sol-gel » associée au « spin coating ». Afrique Science, 2006, 02(3): 245
[36] Doha M H, Alam M J, Rabeya J, et al. Characterization of chemically deposited ZnS thin films on bare and conducting glass. Optik, 2015, 126: 5194
[37] Ongul F, Ulutas U, Yuksel S A, et al. Influences of annealing temperature and thickness on ZnS buffer layers for inverted hybrid solar cells. Synth Metals, 2016, 220: 1
[38] Martínez-Martínez S, May_en-Hern_andez S A, de Moure-Flores F, et al. Sulfiding effects on ZnS thin films obtained by evaporation technique. Vacuum, 2016, 130: 154
[39] Göde F, Gümüş C, Zor M. Investigations on the physical properties of the polycrystalline ZnS thin films deposited by the chemical bath deposition method. J Cryst Growth, 2200, 7
[40] Ates A, Ali Yıldırım M, Kundakcı M, et al. Annealing and light effect on optical and electrical properties of ZnS thin films grown with the SILAR method. Mater Sci Semicond Process, 2007, 10: 281
[41] Ben Achour Z, Ktari T, Ouertani B, et al. Effect of doping level and spray time on zinc oxide thin films produced by spray pyrolysis for transparent electrodes applications. Sens Actuators A, 2007, 134: 447
[42] Farid H, Rafea M A, El-Wahidy E F, et al. Preparation and characterization of ZnS nanocrystalline thin films by low cost dip technique. J Mater Sci: Mater Electron, 2014, 25: 2017
[43] Goktas A, Aslan F, Yasar E, et al. Preparation and characterisation of thickness dependent nano-structured ZnS thin films by sol-gel technique. J Mater Sci: Mater Electron, 2012, 23: 1361